Received: 12 September 2023 | Revised: 11 October 2023 | Accepted: 16 October 2023 | Published online: 17 October 2023

RESEARCH ARTICLE

Archives of Advanced Engineering Science
2023, Vol. 1(1) 27–37
DOI: 10.47852/bonviewAAES32021723

BON VIEW PUBLISHING

Effective Mechanical Properties Evaluation of Unidirectional and Bidirectional Composites Using Virtual Domain Approach at Microscale

Yasser Elmoghazy[1], Elamin Magdi Omer Abuelgasim[1], Seif Ahmed Osman[1], Yazan Rami Hussein Afaneh[1], Omran Mousa Adam Eissa[1] and Babak Safaei[1,*]

[1]*Department of Mechanical Engineering, Eastern Mediterranean University, Türkiye*

Abstract: In this investigation, a 3D micromechanical modeling methodology based on different types of unit cell configuration and representative volume element (RVE) is used to capture the micro-macro mechanical properties of unidirectional (UD) and bidirectional (BD) fiber-reinforced synthetic resin composites. In this regard, hexagonal unit cell and square unit cell were established in order to explore the influence of packing density on representative microstructure properties, considering no effects at the interphase zone between the fiber and the matrix. The virtual geometric generation of 2D-RVE fibers inclusion model process is driven by statistical Monte Carlo simulation algorithm, which is then incorporated into FE solver to develop 3D-BDC RVE laminate model within a virtual scheme. In addition, applying the linear constraint of displacement simulation ensures that the RVE behaves as expected under uniaxial and in-plane loading conditions, leading to more accurate results. This remote constraint helps capture the realistic behaviors of the UD and BD composites models and enables the evaluation of mechanical properties, deformation patterns, and stress distributions within the presented RVE.

Keywords: unit cell, Monte Carlo, representative volume element, linear constraint, unidirectional composites

1. Introduction

Nowadays, composites offer the advantage of tailoring material properties to meet specific requirements such as fiber-reinforced composite that offers the designer the ability to enhance desired mechanical properties including strength, stiffness, thermal conductivity, and electrical conductivity (Faruk et al., 2012; Sundaramoorthy et al., 2023). This versatility allows for the customization of composites to meet a wide range of applications, including structural components (Nwankwo et al., 2023; Tian et al., 2017), thermal/electrical insulation (Mahmud et al., 2023), and medical systems (van Heumen et al., 2008).

To effectively anticipate the effective elastic properties of fiber-reinforced composites, several theoretical and computational models have been put forth by researchers. Moreover, the conventional continuum models cannot directly address the issues raised by heterogeneity nature of composites; hence, micromechanics-based models have been widely employed to address and link the mechanics of materials to their microstructure (Bouaziz et al., 2007; Lee & Simunovic, 2000; Zaïri et al., 2008). Mainly, homogenization and localization are two key approaches used to analyze and predict the mechanical behavior of fiber-reinforced composites and are referred to micro-macro modeling approaches (Esposito et al., 2019; Hassanzadeh-Aghdam et al., 2017; Rafiee & Ghorbanhosseini, 2018; Ullah et al., 2017; Weng et al., 2018). Homogenization modeling simplifies the analysis of fiber-reinforced composites by treating them as homogeneous materials with effective properties, while localization modeling involves the microscale behavior of individual components to predict failure and damage propagations. It is worth mentioning that these two approaches are often used in conjunction to provide a comprehensive understanding of the mechanical behavior of composite materials.

Full-field effective response refers to the behavior of a composite material at macroscopic scale level, considering the microstructure of the material (Kammoun et al., 2011; Würkner et al., 2011). To determine the effective response of a composite material, a virtual approach can be used. This involves modeling a RVE of the composite material subject to various loading conditions to determine effective response of composites with complex microstructures (Ellyin & Xia, 2001; Pan et al., 2008; Xiong et al., 2018). Zaïri et al. (2008); Kim & Lee (2011) developed micromechanical elastic damage model for interfacial damage in fiber-reinforced composites based on RVE considering fiber size dependent. Chen et al. (2019) established homogenization framework for the finite-strain viscoelastic fiber-reinforced composites using Helmholtz-free energy density

*Corresponding author: Babak Safaei, Department of Mechanical Engineering, Eastern Mediterranean University, Türkiye. Email: babak.safaei@emu.edu.tr

© The Author(s) 2023. Published by BON VIEW PUBLISHING PTE. LTD. This is an open access article under the CC BY License (https://creativecommons.org/licenses/by/4.0/).

function conjugated with finite element (FE) modeling. Li et al. (2015) investigated the interface debonding behavior of epoxy glass fiber-reinforced composites caused by curing residual stress using the RVE approach. Catalanotti (2016) developed RVE-based micro-mechanical model for composites reinforced with long fibers using random sequential addition (RSA). Naderi et al. (2017) introduced a computational micromechanics model to explore the failure characteristics of circular and elliptical fiber-reinforced composites under transverse tensile stress conditions. The FE RVE model then incorporated into the UEL subroutine of ABAQUS for the purpose of analyzing 4-node tetrahedron element.

Yang et al. (2022) examined the elastic and viscoelastic properties of short fiber-reinforced composites through the utilization of micromechanical modeling and homogenization techniques. Alhijazi et al. (2021) investigated the elastic properties of nature fiber composites (NFCs) thermosets using RVE with randomly distributed chopped (UD) fiber. Different analytical techniques, including the rule of mixture, Chamis, Halpin-Tsai, and Nielsen methods, were utilized to validate and compare the results obtained from FE analysis. Bisheh (2023) proposed virtual framework to anticipate the elastic properties of UD-NFC based on RVE micromechanical modeling formulation.

Furthermore, Huang and Huang (2020) explored the micromechanical homogenized stresses in RVE of short fibers or particles composites using extended bridging mode. Balasubramani et al. (2022) presented methodological approach for constructing pseudo-random RVE models of UD fiber-reinforced polymer composite at microscale level, including an arbitrary number of fibers and allowing for different aspect ratios. Polyzos et al. (2021) devised multiscale numerical model to determine the elastic characteristics of 3D-printed continuous fiber polymer composites including continuous fibers. Cai et al. (2022) carried out two-step modeling approach to assess the effective properties of microfiber-reinforced composites, considering the presence of primary pores. Tang et al. (2021) studied the longitudinal compression failure mechanisms of continuous carbon fiber-reinforced polymer composites using experimental and computational approaches at micro scale. Recently, Lauff et al. (2023) developed an algorithm to generate continuous short fiber-reinforced composites microstructure with almost planar fiber configurations. Size ratio, fiber length, and directional distributions are only a few of the traits that these artificial microstructures accurately mimic. Yang et al. (2023) predicted the homogeneous properties of long fiber-reinforced composite using RVE based on virtual cluster analysis algorithm.

Further, with a special emphasis on the core fibers' bearing capability, the suggested approach solves a fundamental problem with the accurate distribution of boundary stresses. Li et al. (2023) adopted the discrete element method perspective from the point of view of the displacement field of particles inside fiber-reinforced metal-resin composites under the influence of macroscopic loads.

The three-dimensional implementation is capable of accurately predicting the elastic properties of any continuous fiber-reinforced test composites without relying on any prior assumptions about the behavior of test composites at the macroscale. Here, this virtual model has merely been employed to anticipate the test composite's macro elastic behavior. However, including more accurate constitutive models of the microscale elements, the same framework is anticipated to be extended to predict nonlinear macro-responses of the test composites with imposing periodic boundary conditions.

2. Multiscale Computational Models

2.1 Proposed hexagonal unit cell (HUC) model

HUC that circumscribed inside a circle and the critical point of intersection where the fibers placed taking positions along the edges as shown in Figure 1, the inside angles of the regular hexagonal is 60^0. D_f and s are the diameter of fibers and the radius of the circumscribed circle, respectively; (Rumayshah et al., 2021) this radius is equal to the height edge length of the circumscribed circle and the packing formula can be expressed as:

$$s = D_f \sqrt{\frac{\pi}{2\sqrt{3}\, V_f}} \tag{1}$$

b is the distance of first column of fibers to the central line of fibers arrangements, which is expressed based on s as:

$$b = s\ cos\ 30^0 \tag{2}$$

Figure 1
Hexagonal unit cell packing

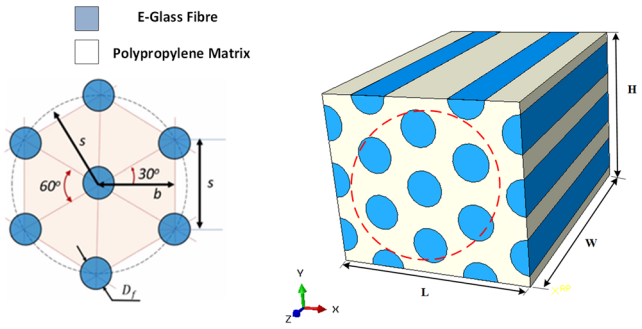

2.1.1. Uniaxial loading case study

First the system covered with representative loading conditions by imposing uniaxial load on all free edges to prevent rigid body motions as illustrated in Figure 2. To be effectively able to extract the stress–strain curve of the proposed model, uniaxial load case along three directions is generated by kinematic linear constraint equation that links the DOF of reference point to all free edges DOFs. In other words, uniaxial loading can be applied parallel to the x, y, and z-axes by specifying a positive displacement on reference point A; a tensile uniaxial load scenario along the x-, y-, or z-axis is generated.

2.1.2. In-plane shear loading case study

Like uniaxial deformation, the specific linear nodal constraints that create simple shear loading are in same manner. In this case, one edge has been assigned zero displacement to prevent rigid body motions. Therefore, the other edges were used to impose the desired shear load case. Figure 3 shows the schematic representation for the shear load cases.

Figure 2
Virtual uniaxial deformation boundary condition of RVE continuous fibres reinforced composite unit cell along (a) x-axes and y-axes and (b) z-axes

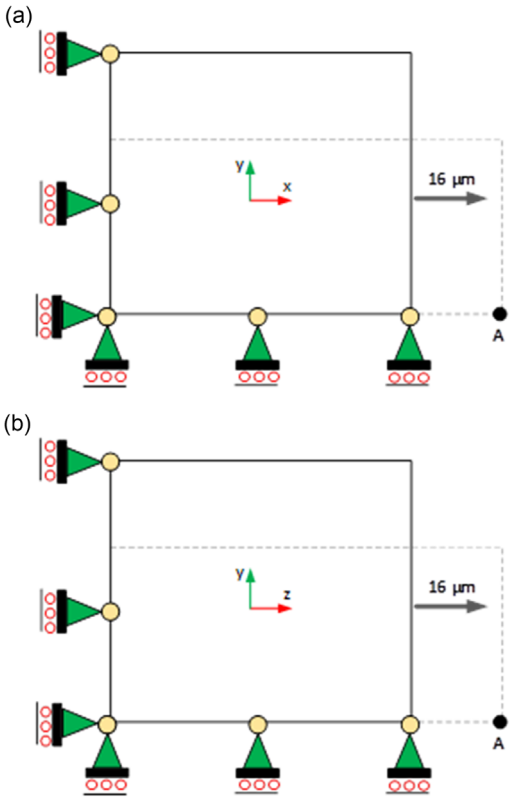

Figure 3
Virtual 2D representation of in-plane shear deformation boundary condition of RVE continuous fibres reinforced composite unit cell

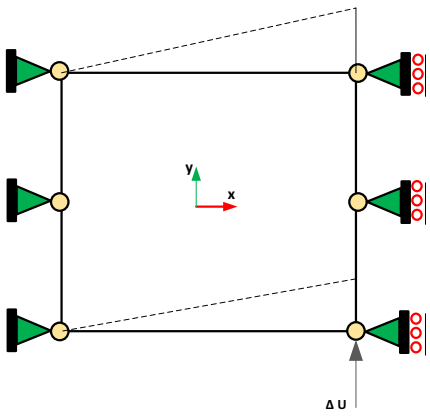

2.2. Proposed square unit cell (SUC) model

The packing of unit cells is a critical aspect of studying periodic structures and composite materials, as it directly influences their mechanical properties and performance. The SUC model provides a representative microstructure as shown in Figure 4, which can be employed to investigate packing arrangements. The SUC offers

Figure 4
Constriction of geometrical arrangement of UDC square unit cell

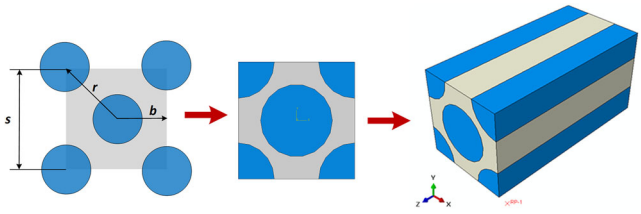

a symmetric geometry that simplifies the analysis of packing arrangements and allows for efficient utilization of computational modeling. The packing formula can be expressed as (Rumayshah et al., 2021)

$$s = D_f \sqrt{\frac{\pi}{2\,V_f}} \tag{3}$$

From Figure 4, the distance from the central line of fibers arrangements to the edge of the unit cell b is expressed based on s as

$$b = 0.5\,s \tag{4}$$

$$r = s\ \cos\ 45^0 \tag{5}$$

2.3. Proposed RVE modeling of bidirectional (BD) composite

BD composite in the sense that the laminates are oriented in a 0° and 90° direction. proposed for BDC RVE model considered a 0° degree outer layers and two 90° inside layers making a stacking sequence is $[0^\circ/90^\circ/90^\circ/0^\circ] = [0^\circ/90^\circ]$ plies as shown in Figure 5(a). Those laminate arrangements are always balanced so that they are symmetric about the central line to assure the balance of mechanical properties; thus, buckling can be avoided.

A 3D-RVE was derived from the 2D-RVE obtained using the Monte Carlo algorithm within ABAQUS CAE software by extruding the 2D-RVE in out-of-plane direction to form the 3D-RVE. Then, inputs from Monte Carlo algorithm were passed onto ABAQUS using a Python script developed for this purpose.

Figure 5
(a) Staking sequences of proposed BDC RVE with random fibers distribution. (b) 3D model of BDC RVE in virtual domain

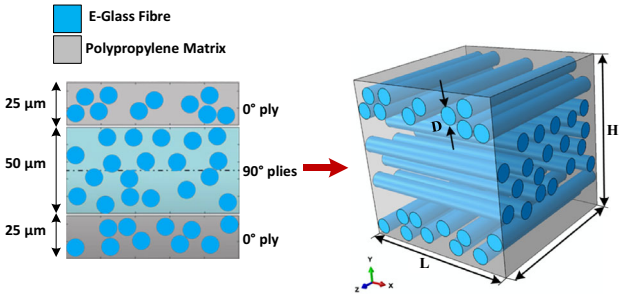

3. Virtual Geometric RVE Modeling

It is widely known that an appropriate RVE must first be identified to analyze a composite material using micromechanics while the effects of interface boundaries can be neglected since the fibers and the resin matrix are perfectly bonded together (Mortell et al., 2017; Vaughan & McCarthy, 2010). The number of fibers N fit the model can be calculated based on volume fraction, width, and diameter of the fibers as follows:

$$N = \frac{4V_f WH}{\pi D^2_f} \tag{6}$$

where V_f, W, H, and D_f are fiber volume fraction, width, height, and diameter of the proposed RVE model, respectively. This work employed the well-known Monte Carlo approach for generating random fibers inclusions within the proposed 2D-RVE domain including overlap, edge fibers, and periodicity design criteria. In this manner, the algorithm keeps adding fibers following the design criteria until necessary volume fraction is reached. The procedure steps can explain in detail as following:

1. Define RVE Characteristics: Begin by specifying the characteristics of the desired RVE. This includes the dimensions of the RVE, the types of particles to be packed, their size distribution, and any constraints or interactions between the particles.
2. Initialize Empty RVE: Create an empty 3D grid or container representing the RVE. Then, randomly generate fibers according to the defined size distribution using the RSA algorithm.
3. Random Placement: Select a random position within the empty RVE to place the generated particle. The position should be such that the particle is fully contained within the RVE and does not overlap with any existing particles.

- **Overlap Check:** Perform an overlap check to ensure that the newly generated particle does not overlap with any previously placed particles. This is typically done by checking for intersection between the generated particle and all existing particles in the RVE window if an overlap is detected, discard the particle, and go back to step 3 to generate a new particle.
- **Non-overlapping Placement:** If the newly generated particle passes the overlap check, place it in the selected position within the RVE. Repeat steps 3–6: Repeat steps 3–6 until the desired number of particles or the desired packing density is achieved.
- **Monte Carlo Iterations:** Perform multiple Monte Carlo iterations to refine the packing. In each iteration, randomly select a particle within the RVE and attempt to move it to a new random position while ensuring that it does not overlap with other particles. Accept or reject the move based on a Metropolis criterion or another acceptance rule, which helps improve the packing quality.
- **Repeat Monte Carlo Iterations:** The Monte Carlo iterations repeated with different steps to allow for particle rearrangements and better packing quality. The number of iterations depends on the desired level of packing optimization.
- **Final RVE Output:** Once the desired number of iterations is reached, the final configuration of particles represents the 3D RVE based on the Monte Carlo implementation of the RSA algorithm. When conducting finite element (FE) simulations of 3D-BDC RVE laminates in Abaqus, for mesh modeling, a 3D FE model was built using FE software Abaqus®, by using -20 node continuum quadratic brick element C3D20® to discretize the RVE model using sizing control technique with maximum mesh global size of 10 μm and maximum deviation factor of 0.1 as depicted in Figure 6. The flow chart of micromechanical modeling methodology for 3D RVE is shown in Figure 7. It is necessary to apply linear constraints to capture the micro response of the proposed composites and enforce boundary conditions and other constraints on the RVE model. These constraints are typically applied to control displacements, rotations, or forces at specific nodes or surfaces of the model. By properly applying linear constraints, the FE simulation can replicate the real-world behavior of the UD RVE more realistically. This ensures that the response of the material within the RVE accurately reflects its macroscopic behavior. Furthermore, the linear constraint of displacement is a boundary condition that is commonly applied in finite element (FE) simulations to control the movement or displacement of nodes in a model. It ensures that certain nodes or face surfaces within the model are constrained in a specific manner. The following equation explains the linear displacement constraint mechanism as shown in Figure 8:

Figure 6
FE mesh mode of the proposed BDC RVE l in Abaqus with C3D20® mesh element

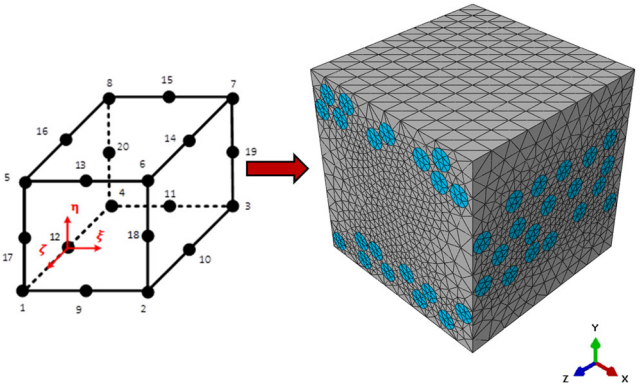

$$U(x)^{x-front} = U(x)^{RP-front-face} \tag{7}$$

$$U(y)^{y-front} = U(y)^{RP-top-face} \tag{8}$$

$$U(z)^{z-front} = U(z)^{RP-top-face} \tag{9}$$

To comprehensively predict the macro elastic behaviors of the glass fiber-reinforced composites subjected to linear displacement-control as indicated above, the effective macroscale E_{ij}, G_{ij} Young's modulus, and rigidity modulus within 3D RVE domain, respectively, can obtain through homogenization approach as follows (Danielsson et al., 2002):

$$\sigma_{ij} = \frac{1}{V}\int \sigma_{micro} dV \tag{10}$$

$$\varepsilon_{ij} = \frac{1}{V}\int \varepsilon_{micro} dV \tag{11}$$

4. Results and Discussion

In this section, 3D unit cell of hexagonal and square configuration UDC models were used. The model was exposed to

Figure 7
Flow chart of micromechanical modeling methodology for 3D RVE creation based on the Monte Carlo implementation of RSA algorithm

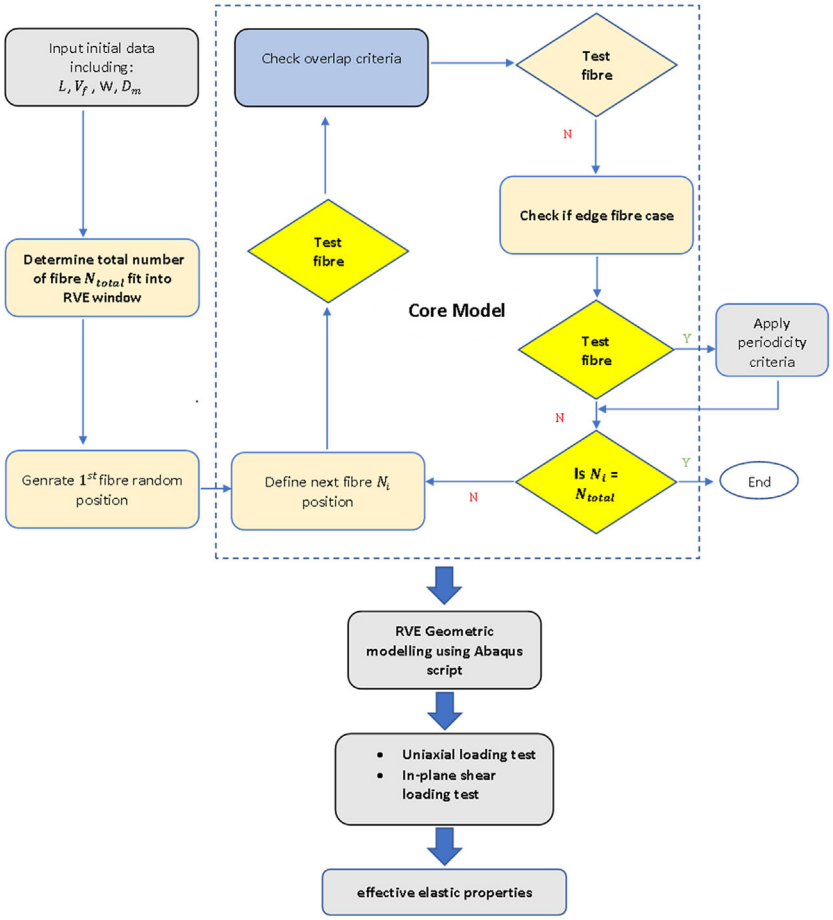

Figure 8
Representation of how periodically boundary condition applied uniaxial and in-plane shear through BD laminate RVE using linear constraint that link with reference point (120, 0, 100) μm

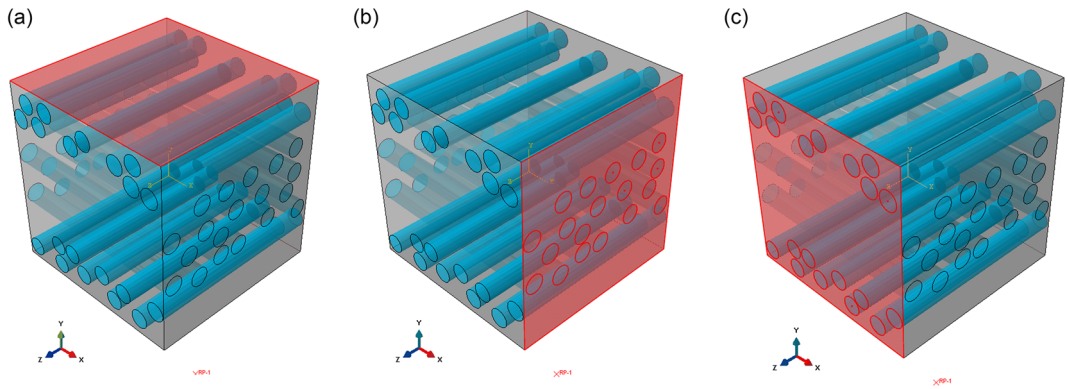

uniaxial tensile and in-plane shear deformation in specified load scenarios. The fibers in this study were considered to be an isotropic linear elastic material made of E-glass, whereas the matrix material was composed of polypropylene. The geometrical and material properties of proposed multiscale computational models are shown in Table 1. The stress–strain curve of the three proposed model for different loading scenarios is depicted in Figure 9. The plastic deformation (PE) contours of HUC are shown in Figures 10 and 11. Figure 12 shows contour plots of uniaxial tensile PE with respect to σ_{xx} and σ_{yy} and average Von Mises σ_{zz}, for 3D SUC polypropylene continuous E-glass fiber reinforced while Figure 13 explains PE strain and in-plane shear stress

Table 1
Geometrical and material properties of proposed multiscale computational models (Daniel, 1996)

Parameter		HUC	SUC	BDC-RVE
D (μm)		15	15	15
V_f		0.3	0.6	0.3
s (μm)		24.15	24.27	–
b (μm)		20.91	12.13	–
Length of RVE (μm)		83.6426	24.27	100
Width of RVE (μm)		72.436	24.27	100
Height of RVE (μm)		120	24.27	100
Young modulus (Gpa)	E_f=73, E_m=1.308			
Poisson ratio	ν_f=0.2, ν_m=0.43			
Density (m^3/kg)	ρ_f=1450, ρ_m= 903			

for 3D SUC composites considering applied nominal strain of 0.01 comparative analysis and reiterating the significance of the virtual algorithm as a valuable tool for predicting the effective elastic constant E_{zz} of composites with a high degree of accuracy and practicality. The present model exhibits an error of 0.7% compared to the analytical mode as shown in Table 2.

In Abaqus, the uniaxial and shear boundary conditions are applied to simulate a UDC laminates RVE; results are shown in Figures 14 and 15. This allows the analysis of a smaller

Table 2
Current study compares the estimated effective elastic constant E_{zz} of a SUC-UD fiber-reinforced synthetic resin composites with a fiber volume fraction of 0.6 using analytical model, and virtual algorithm approach proposed in this study

Effective modulus (Gpa)	Present SUC	Rule of mixtures (Bisheh, 2023)	Relative error
E_{zz}	44	44.32	0.7%

Figure 9
Schematic illustration of stress–strain curves for (a) SUC-UD composite. (b) HUC-UD composite. (c) RVE-BD composite with stacking sequence [0/90/90/0]

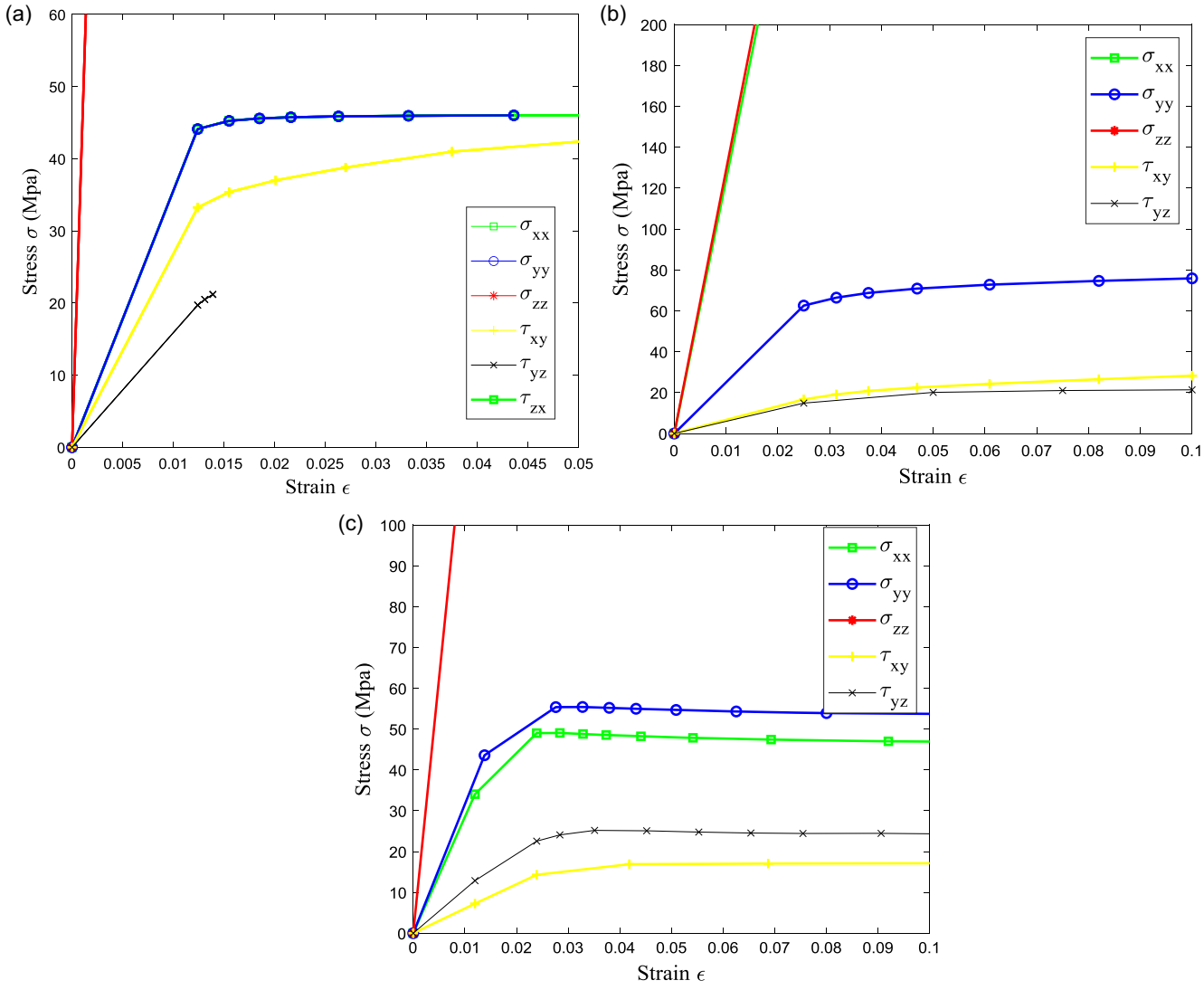

Figure 10
PE with respect to (a) σ_{xx}, (b) σ_{yy}, and (c) σ_{zz} for 3D HUC polypropylene continuous E-glass fiber reinforced based

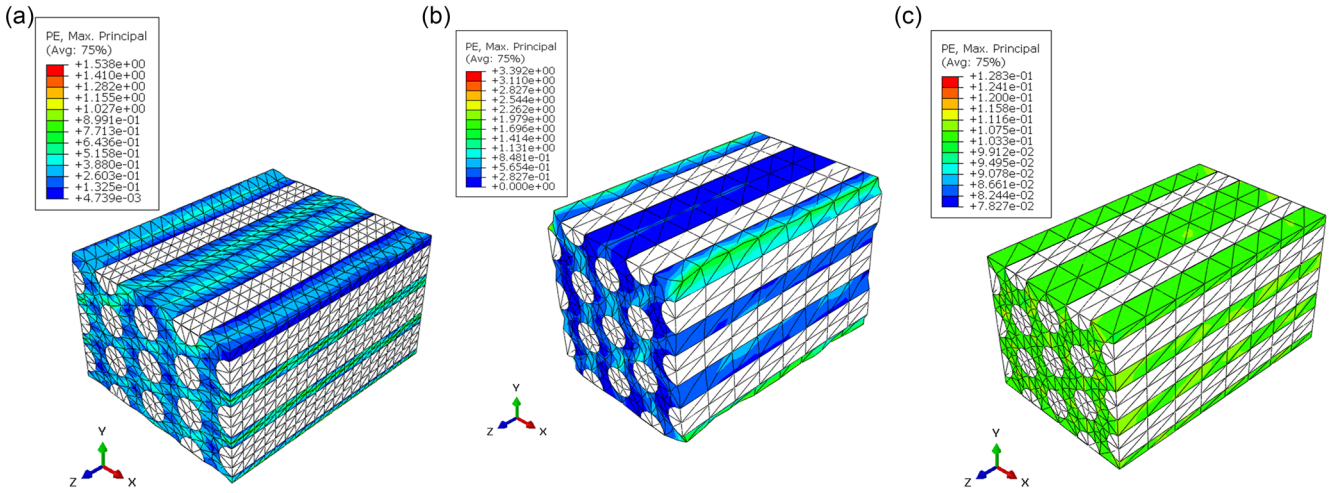

Figure 11
PE strain contour plots illustrating in-plane shear PE with respect (a) τ_{xy} and (b) τ_{zx} (c) τ_{yz} for 3D SUC polypropylene continuous E-glass fiber reinforced based

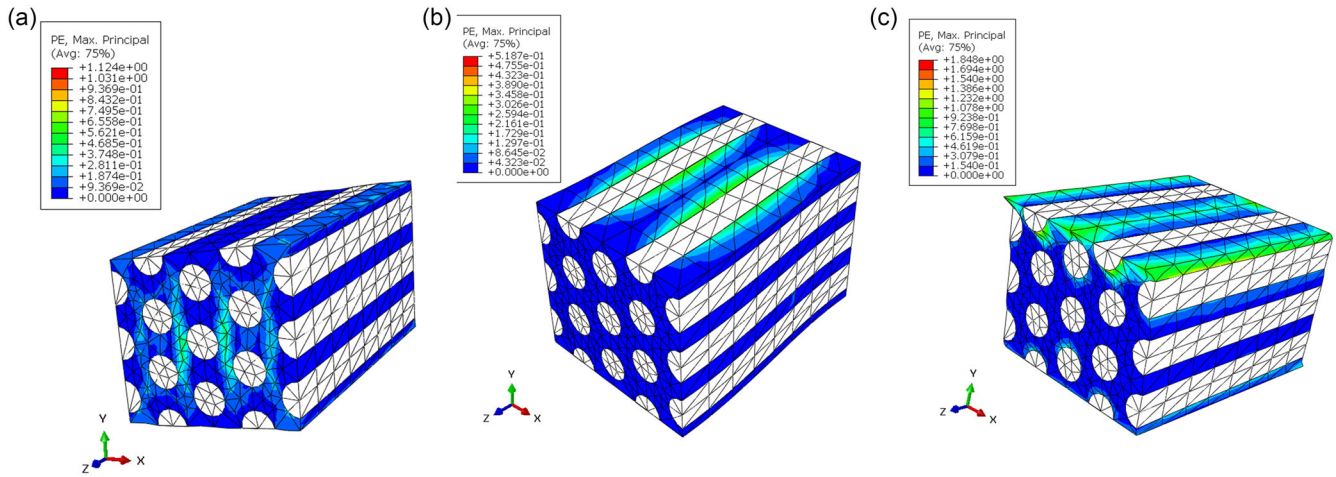

Figure 12
Contour plots illustrating uniaxial PE with respect to (a) σ_{xx} and (b) σ_{yy} for 3D SUC polypropylene continuous E-glass fiber reinforced based (c) contour plots of average Von Mises σ_{zz}

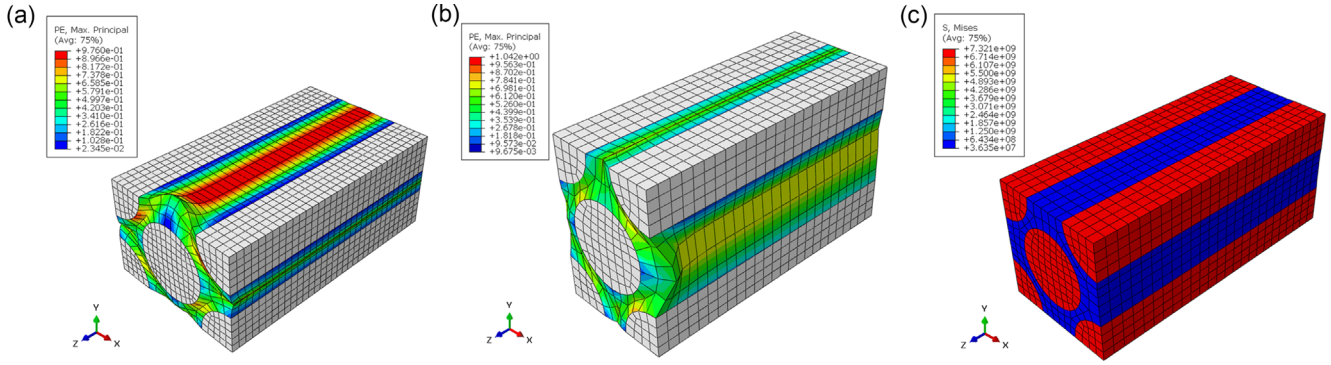

Figure 13
PE strain contour plots illustrating in-plane shear PE with respect to (a) γ_{xy} and (b). γ_{yz} for 3D HUC polypropylene continuous E-glass fiber reinforced based

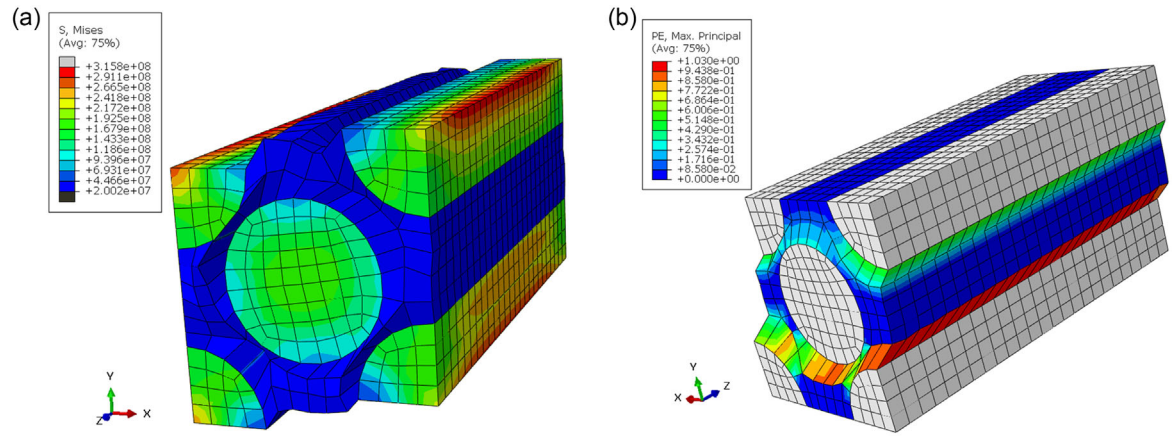

Figure 14
PE contour plots illustrating uniaxial PE with respect to (a) σ_{xx}, (b) σ_{yy}, and (c) σ_{zz} for 3D-DBC RVE polypropylene continuous E-glass fiber reinforced based

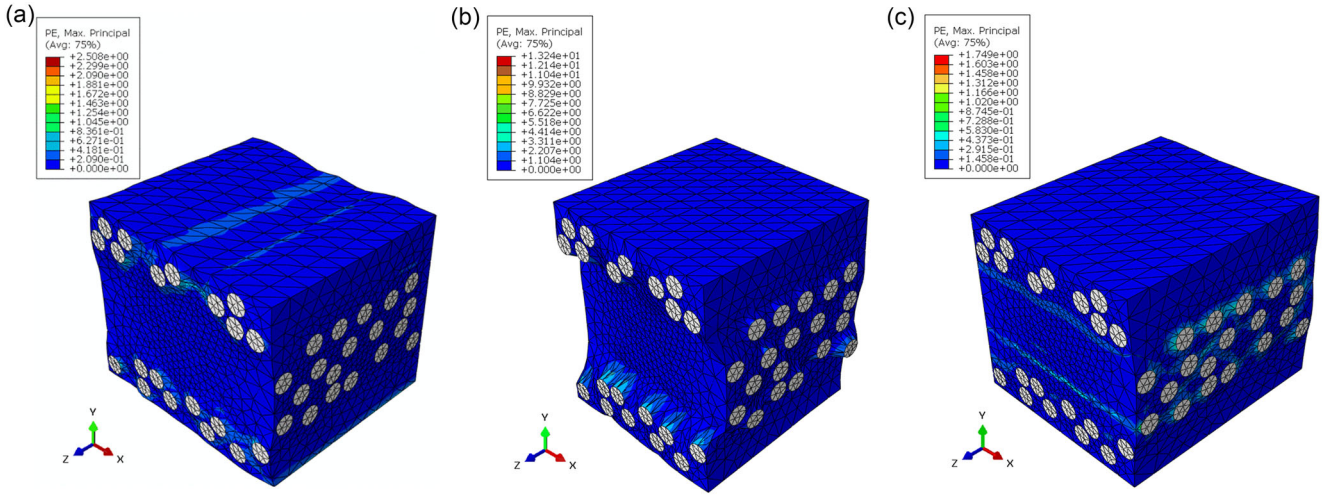

Figure 15
PE contour plots illustrating uniaxial PE with respect to (a) τ_{xy}, (b) τ_{zx}, and (c) τ_{yz} for 3D-DBC RVE polypropylene continuous E-glass fiber reinforced based

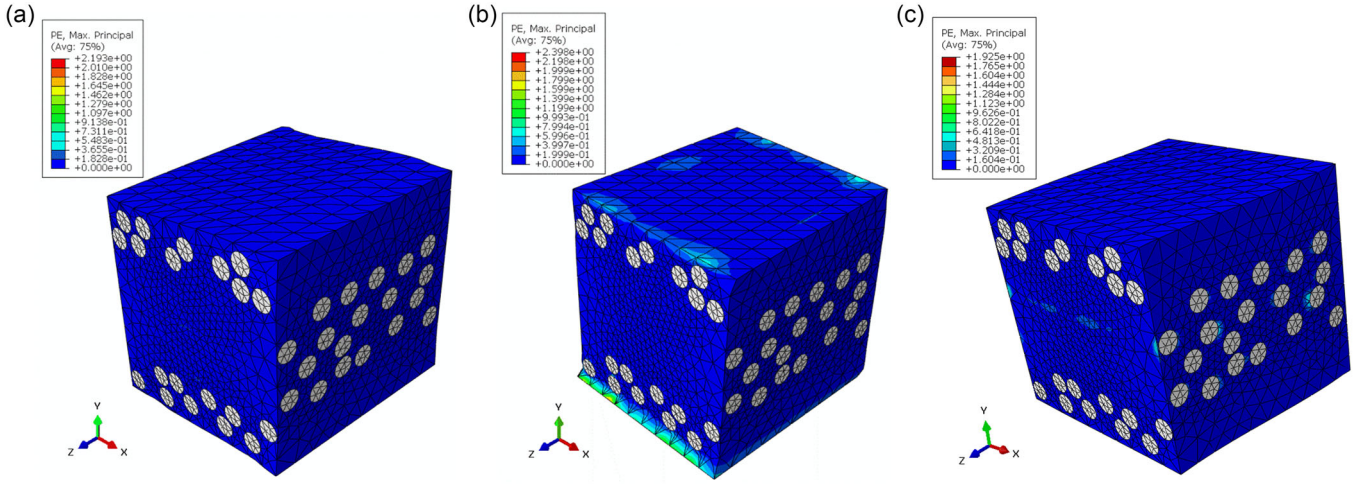

representative portion of a larger structure or material, reducing computational costs while still capturing the overall behavior accurately. Here, an explanation of how the RVE periodic boundary condition is applied in Abaqus is shown. First, the RVE geometry created the geometry of the RVE using Abaqus' modeling capabilities. This can involve defining the solid elements, surfaces, and edges that represent the RVE. After that, Established RVE Periodicity: Identify the boundaries of the RVE that will have periodicity. Typically, these are opposite faces or edges of the RVE that should exhibit the same displacement, stress, or strain conditions. Create a Reference Point: Select a point within the RVE that will serve as a reference for the boundary condition. This point should ideally be located away from any areas with high strain gradients or stress concentrations.

Create the Analysis Model: Define the material properties, loads, and constraints for the RVE analysis. This involves assigning appropriate material models, defining boundary conditions, and applying loads to the RVE geometry.

Solve the Analysis: Run the analysis in Abaqus to obtain the response of the RVE. Abaqus will automatically enforce the periodicity defined in the previous steps and calculate the behavior of the RVE based on the applied loading conditions.

Post-processing: Analyze the results obtained from the RVE analysis to extract the desired information. Abaqus provides various post-processing tools to visualize and interpret the results, such as contour plots, stress–strain curves, and displacement fields. This approach enables the analysis of a smaller portion of a larger structure or material, reducing computational effort while still capturing the overall behavior accurately. Typical comparisons of effective mechanical moduli of the proposed models UD and BD composite with different volume fraction are shown in Table 3. It can be observed that both HUC and BD-RVE, which contain same volume fraction of $V_f = 30\%$, have almost same effective moduli E_{yy}, E_{zz}, and G_{xy}, but BD-RVE shows more stiffness in x-axes tensile direction.

Table 3
Comparisons of effective properties of the proposed models UD and BD composite with different volume fraction

Effective modulus (Gpa)	SUC	HUS	DBC RVE
E_{zz}	3.57	2.05	11.88
E_{yy}	3.57	2	2.50
E_{zz}	43.94	12.5	13
G_{xy}	2.69	0.61	0.67
G_{yz}	1.61	1.08	0.59
G_{xz}	2.55	0.4	0.74

5. Conclusion

In this study, the paking density of different unit cell configrations and their effects on the micro-macro mechanical response of UDC were studied. Further, a random fibers inclusion was realistically created within a virtual RVE composite domain using Monte Carlo simulation within FE analysis scheme, considering uniaxial and shear loading conditions. Afterwards, the use of the Monte Carlo algorithm, in conjunction with RSA, was employed to generate a randomized arrangement of fibers considering periodicity criteria of fibers to estimate the effective engineering characteristics using numerical simulation technique. The simulation results of a PE behaviors of proposed multiscale computational models were plotted in order to effectively observe the micro-macro mechanical response using averaging volume homogenization approach. It was noticed that the mechanical properties of composite materials can be strengthened by providing a different design that integrates different laminations of basic RVE models. To elucidate the effectiveness of the proposed method, SUC model was validated against the rule of mixture analytical model so that the proposed model effectively captures the macro-effective elastic properties of UD composites. In general, using the proposed methodology described in this paper, the evolution of damage plastic failure in UD and BD composites can be modeled to provide valuable insights for improving the design of composite materials; hence, the methodology can be extended in the future to investigate the vibration behaviors of sandwich structures containing fiber-reinforced synthetic resin composites.

Conflicts of Interest

Babak Safaei is the Editor-in-Chief for *Archives of Advanced Engineering Science*, and was not involved in the editorial review or the decision to publish this article. The authors declare that they have no conflicts of interest to this work.

References

Alhijazi, M., Safaei, B., Zeeshan, Q., & Asmael, M. (2021). Modeling and simulation of the elastic properties of natural fiber-reinforced thermosets. *Polymer Composites, 42*, 3508–3517. https://doi.org/10.1002/PC.26075

Balasubramani, N. K., Zhang, B., Chowdhury, N. T., Mukkavilli, A., Suter, M., & Pearce, G. M. (2022). Micro-mechanical analysis on random RVE size and shape in multiscale finite element modelling of unidirectional FRP composites. *Composite Structures*, *282*. https://doi.org/10.1016/J.COMPSTRUCT.2021.115081

Bisheh, H. (2023). Uncertainty analysis for prediction of elastic properties of unidirectional bamboo fiber-reinforced composites. *Structures*, *54*, 198–220. https://doi.org/10.1016/J.ISTRUC.2023.05.032

Bouaziz, A., Zaïri, F., Naït-Abdelaziz, M., Gloaguen, J. M., & Lefebvre, J. M. (2007). Micromechanical modelling and experimental investigation of random discontinuous glass fiber polymer–matrix composites. *Composites Science and Technology*, *67*, 3278–3285. https://doi.org/10.1016/J.COMPSCITECH.2007.03.031

Cai, H., Ye, J., Shi, J., Wang, Y., Shi, Y., Huang, B., . . . , & Ye, J. (2022). A new two-step modeling strategy for random micro-fiber reinforced composites with consideration of primary pores. *Composites Science and Technology*, *218*. https://doi.org/10.1016/J.COMPSCITECH.2021.109122

Catalanotti, G. (2016). On the generation of RVE-based models of composites reinforced with long fibres or spherical particles. *Composite Structures*, *138*, 84–95. https://doi.org/10.1016/J.COMPSTRUCT.2015.11.039

Chen, Y., Guo, Z., Gao, X. L., Dong, L., & Zhong, Z. (2019). Constitutive modeling of viscoelastic fiber-reinforced composites at finite deformations. *Mechanics of Materials*, *131*, 102–112. https://doi.org/10.1016/J.MECHMAT.2019.02.001

Daniel, M. I. (1996). Engineering mechanics of composite materials. *Mater Des, 17*, 114. https://doi.org/10.1016/s0261-3069(97)87195-6.

Danielsson, M., Parks, D.M., & Boyce, M.C. (2002). Three-dimensional micromechanical modeling of voided polymeric

materials. *Journal of the Mechanics and Physics of Solids*, *50*, 351–379. https://doi.org/10.1016/S0022-5096(01)00060-6

Ellyin, F., & Xia, Z. (2001). Rate-dependent constitutive modelling and micro-mechanical analysis of fibre-reinforced metal–matrix composites. *Journal of the Mechanics and Physics of Solids*, *49*, 2543–2555. https://doi.org/10.1016/S0022-5096(01)00067-9

Esposito, L., Cutolo, A., Barile, M., Lecce, L., Mensitieri, G., Sacco, E., & Fraldi, M. (2019). Topology optimization-guided stiffening of composites realized through automated fiber placement. *Composites Part B: Engineering*, *164*, 309–323. https://doi.org/10.1016/J.COMPOSITESB.2018.11.032

Faruk, O., Bledzki, A. K., Fink, H. P., & Sain, M. (2012). Biocomposites reinforced with natural fibers: 2000–2010. *Progress in Polymer Science*, *37*, 1552–1596. https://doi.org/10.1016/J.PROGPOLYMSCI.2012.04.003

Hassanzadeh-Aghdam, M. K., Ansari, R., & Darvizeh, A. (2017). Micromechanical modeling of thermal expansion coefficients for unidirectional glass fiber-reinforced polyimide composites containing silica nanoparticles. *Composites Part A: Applied Science and Manufacturing*, *96*, 110–121. https://doi.org/10.1016/J.COMPOSITESA.2017.02.015

Huang, H. B., & Huang, Z. M. (2020). Micromechanical prediction of elastic-plastic behavior of a short fiber or particle reinforced composite. *Composites Part A: Applied Science and Manufacturing*, *134*. https://doi.org/10.1016/J.COMPOSITESA.2020.105889

Kammoun, S., Doghri, I., Adam, L., Robert, G., & Delannay, L. (2011). First pseudo-grain failure model for inelastic composites with misaligned short fibers. *Composites Part A: Applied Science and Manufacturing*, *42*, 1892–1902. https://doi.org/10.1016/J.COMPOSITESA.2011.08.013

Kim, B. R., & Lee, H. K. (2011). Elastic-damage modeling for particulate composites considering cumulative damage. *Int J Damage Mech, 20*, 131–158. https://doi.org/10.1177/1056789509346688

Lauff, C., Schneider, M., Montesano, J., & Böhlke, T. (2023). An orientation corrected shaking method for the microstructure generation of short fiber-reinforced composites with almost planar fiber orientation. *Composite Structures*, *322*. https://doi.org/10.1016/J.COMPSTRUCT.2023.117352

Lee, H. K., & Simunovic, S. (2000). Modeling of progressive damage in aligned and randomly oriented discontinuous fiber polymer matrix composites. *Composites Part B: Engineering*, *31*, 77–86. https://doi.org/10.1016/S1359-8368(99)00070-0

Li, J., Liu, X., Yao, X., & Yuan, Y. (2015). A micromechanical debonding analysis of fiber-reinforced composites due to curing residual stress. *Journal of Reinforced Plastics and Composites*, *34*, 962–971. https://doi.org/10.1177/0731684415584952

Li, Y., Xin, J., Li, W., & Huang, H. (2023). Meso-scale characterization and discrete element simulation of fiber-reinforced resin-mineral composite. *Computational Particle Mechanics*, 1–12. https://doi.org/10.1007/S40571-023-00573-2

Mahmud, M. A., Abir, N., Anannya, F. R., Nabi Khan, A., Rahman, A. N. M. M., & Jamine, N. (2023). Coir fiber as thermal insulator and its performance as reinforcing material in biocomposite production. *Heliyon*, *9*. https://doi.org/10.1016/J.HELIYON.2023.E15597

Mortell, D. J., Tanner, D. A., & McCarthy, C. T. (2017). A virtual experimental approach to microscale composites testing. *Composite Structures*, *171*, 1–9. https://doi.org/10.1016/J.COMPSTRUCT.2017.03.016

Naderi, M., Apetre, N., & Iyyer, N. (2017). Effect of interface properties on transverse tensile response of fiber-reinforced composites: Three-dimensional micromechanical modeling. *Journal of Composite Materials*, *51*, 2963–2977. https://doi.org/10.1177/0021998316681189

Nwankwo, C. O., Mahachi, J., Olukanni, D. O., & Musonda, I. (2023). Natural fibres and biopolymers in FRP composites for strengthening concrete structures: A mixed review. *Construction and Building Materials*, *363*. https://doi.org/10.1016/J.CONBUILDMAT.2022.129661

Pan, Y., Iorga, L., & Pelegri, A. A. (2008). Analysis of 3D random chopped fiber reinforced composites using FEM and random sequential adsorption. *Computational Materials Science*, *43*, 450–461. https://doi.org/10.1016/J.COMMATSCI.2007.12.016

Polyzos, E., Van Hemelrijck, D., & Pyl, L. (2021). Numerical modelling of the elastic properties of 3D-printed specimens of thermoplastic matrix reinforced with continuous fibres. *Composites Part B: Engineering*, *211*. https://doi.org/10.1016/J.COMPOSITESB.2021.108671

Rafiee, R., & Ghorbanhosseini, A. (2018). Predicting mechanical properties of fuzzy fiber reinforced composites: Radially grown carbon nanotubes on the carbon fiber. *International Journal of Mechanics and Materials in Design*, *14*, 37–50.

Rumayshah, K. K., Dirgantara, T., Judawisastra, H., & Wicaksono, S. (2021). Numerical micromechanics model of carbon fiber-reinforced composite using various periodical fiber arrangement. *J Mech Sci Technol, 35*, 1401–6. https://doi.org/10.1007/s12206-021-0306-9

Sundaramoorthy, E., Mahanwar, P. A., Patil, J., & Mundhe, G. (2023). Polyolefin fiber, polyolefin fiber reinforced composites and their applications: A review. *Journal of Polymer Engineering, 43*, 219–230.

Tang, H., Sun, Q., Li, Z., Su, X., & Yan, W. (2021). Longitudinal compression failure of 3D printed continuous carbon fiber reinforced composites: An experimental and computational study. *Composites Part A: Applied Science and Manufacturing*, *146*. https://doi.org/10.1016/J.COMPOSITESA.2021.106416

Tian, H., Cui, Y. H., Zhang, Y. X., & Yang, C. (2017). The application of general self-consistent model on mechanical behaviour of fibre-reinforced cementitious composites. *Construction and Building Materials*, *146*, 114–121. https://doi.org/10.1016/J.CONBUILDMAT.2017.04.045

Ullah, Z., Kaczmarczyk, L., & Pearce, C. J. (2017). Three-dimensional nonlinear micro/meso-mechanical response of the fibre-reinforced polymer composites. *Composite Structures, 161*, 204–214. https://doi.org/10.1016/J.COMPSTRUCT.2016.11.059

van Heumen, C. C. M., Kreulen, C. M., Bronkhorst, E. M., Lesaffre, E., & Creugers, N. H. J. (2008). Fiber-reinforced dental composites in beam testing. *Dental Materials*, *24*, 1435–1443. https://doi.org/10.1016/J.DENTAL.2008.06.006

Vaughan, T. J., & McCarthy, C. T. (2010). A combined experimental–numerical approach for generating statistically equivalent fibre distributions for high strength laminated composite materials. *Composites Science and Technology*, *70*, 291–297. https://doi.org/10.1016/J.COMPSCITECH.2009.10.020

Weng, J., Wen, W., Cui, H., & Chen, B. (2018). Micromechanical analysis of composites with fibers distributed randomly over the transverse cross-section. *Acta Astronautica*, *147*, 133–140. https://doi.org/10.1016/J.ACTAASTRO.2018.03.056

Würkner, M., Berger, H., & Gabbert, U. (2011). On numerical evaluation of effective material properties for composite structures with rhombic fiber arrangements. *International Journal of Engineering Science*, *49*, 322–332. https://doi.org/10.1016/J.IJENGSCI.2010.12.016

Xiong, X., Hua, L., Miao, M., Shen, S. Z., Li, X., Wan, X., Guo, W. (2018). Multi-scale constitutive modeling of natural fiber fabric reinforced composites. *Composites Part A: Applied Science and Manufacturing, 115*, 383–396. https://doi.org/10.1016/J.COMPOSITESA.2018.10.016

Yang, P., Chen, Y., Guo, Z., Hu, N., & Sun, W. (2022). Modeling the effective elastic and viscoelastic properties of randomly distributed short fiber reinforced composites. *Composites Communications*, *35*. https://doi.org/10.1016/J.COCO.2022.101341

Yang, Y., Liu, T., Aliabadi, M. H., & Tang, S. (2023). Virtual clustering analysis for long fiber reinforced composites. *Computational Mechanics*, *71*, 1139–1159.

Zaïri, F., Naït-Abdelaziz, M., Gloaguen, J. M., Bouaziz, A., & Lefebvre, J. M. (2008). Micromechanical modelling and simulation of chopped random fiber reinforced polymer composites with progressive debonding damage. *International Journal of Solids and Structures*, *45*(20), 5220–5236. https://doi.org/10.1016/j.ijsolstr.2008.05.013

How to Cite: Elmoghazy, Y., Abuelgasim, E. M.O., Osman, S. A., Afaneh, Y. R.H., Eissa, O. M.A., & Safaei, B. (2023). Effective Mechanical Properties Evaluation of Unidirectional and Bidirectional Composites Using Virtual Domain Approach at Microscale. *Archives of Advanced Engineering Science* 1(1), 27–37, https://doi.org/10.47852/bonviewAAES32021723